



Supercritical water gasification of organic acids and alcohols: The effect of chain length

Anand G. Chakinala^{a,*}, Shushil Kumar^a, Andrea Kruse^b, Sascha R.A. Kersten^a, Wim P.M. van Swaij^a, D.W.F. (Wim) Brilman^a

^a Thermo-Chemical Conversion of Biomass (TCCB), Faculty of Science and Technology, University of Twente, P.O. Box 217, 7500 AE Enschede, The Netherlands

^b Institute of Catalysis Research and Technology, Karlsruhe Institute of Technology, Hermann-von-Helmholtz-Platz 1, 76344 Eggenstein-Leopoldshafen, Germany

ARTICLE INFO

Article history:

Received 28 February 2012

Received in revised form

22 November 2012

Accepted 23 November 2012

Keywords:

Supercritical water gasification

Acids

Alcohols

Chain length

ABSTRACT

We report the influence of the molecular structure on the gasification behaviour for a homologous series of linear chain (C₁–C₈) carboxylic acids and alcohols in supercritical water (600 °C and 250 bar) at two different concentrations (10 and 20 wt%). The initial concentration of carboxylic acids had a significant influence on the gasification efficiency (GE), whereas no such effect was found for the alcohol series studied. Alcohols were found to be much easier to gasify than the organic acids and the carbon GE trend of alcohols was opposite to that of acids, especially for the short chain compounds. With increasing chain length the GE stabilizes to around 50% at the conditions chosen. From gas and liquid phase product analysis decomposition schemes were proposed for the short chain compounds.

A remarkable oscillatory behaviour of the methane and CO₂ product yield with increasing chain length of the acids and alcohols was found experimentally. A simple model was derived, based on essentially a β-scission cracking mechanism, which was able to explain the observed product spectrum and the oscillatory behaviour. Additionally, the influence of the number and positioning of OH groups on the gasification behaviour was studied.

© 2012 Elsevier B.V. All rights reserved.

1. Introduction

Supercritical water (SCW), water heated under pressure to above its critical point ($T > 374$ °C, $P > 220$ bar), is attracting attention as a medium for chemical reactions [1–3]. Supercritical water gasification (SCWG) has been growing as a promising technology in converting (residual) organics present in aqueous biomass/waste streams with a high water content (80%) to high heating value product gases (e.g., H₂, CH₄, CO) and clear water [4–7]. A key advantage of the SCW is the possibility of tuning the properties of the reaction medium by varying the pressure and temperature and thus optimizing the reaction conditions [4,8]. The water content in the aqueous biomass streams serves the purposes of reaction medium, being a reactant and act as a catalyst for the enhanced degradation rates of the organics in the biomass. However, the decomposition pathways of real biomass differs in sub- and supercritical water (ionic- vs. radical reactions being dominating) and is influenced by several variables such as feed characteristics (type of organics, solids/dry matter like cell walls,

etc.) and process conditions (temperature, pressure, initial feed concentration, reaction time, heating up rate, pH) [2,4].

Several intermediate compounds are formed during the course of reaction when biomass is heated up under hydrothermal conditions, the majority of the stable intermediate compounds being similar to the compounds found in the hydrothermal liquefaction [4]. These intermediate compounds constitute of alcohols, acids, aldehydes, diols, ketones, phenols, furfurals and several other compounds [4]. Some of these compounds convert readily into gases (desired reaction), but additionally some of these compounds may also undergo polymerization reactions, leading to the formation of less reactive char/coke, which ultimately reduces the gas yield and can even result in reactor plugging [5].

From earlier reports and our own unpublished data it is known that some compounds (for e.g., methanol) are not very reactive in SCW in the absence of any catalyst and do not lead to char/tar formation [11–14]. However, other, often larger, compounds such as glucose and biomass feed containing sugar compounds are more reactive, and rapidly lead to char/tar formation [2,5]. It is therefore essential to understand more of the chemistry of biomass gasification in supercritical water in terms of the gasification behaviour; e.g., on the role of different functional groups and chain length effects. For future development this may help to minimize the char/tar formation and increase the carbon to gas conversion/gas

* Corresponding author. Tel.: +31 53 489 2141; fax: +31 53 489 4738.

E-mail address: a.g.chakinala@gmail.com (A.G. Chakinala).

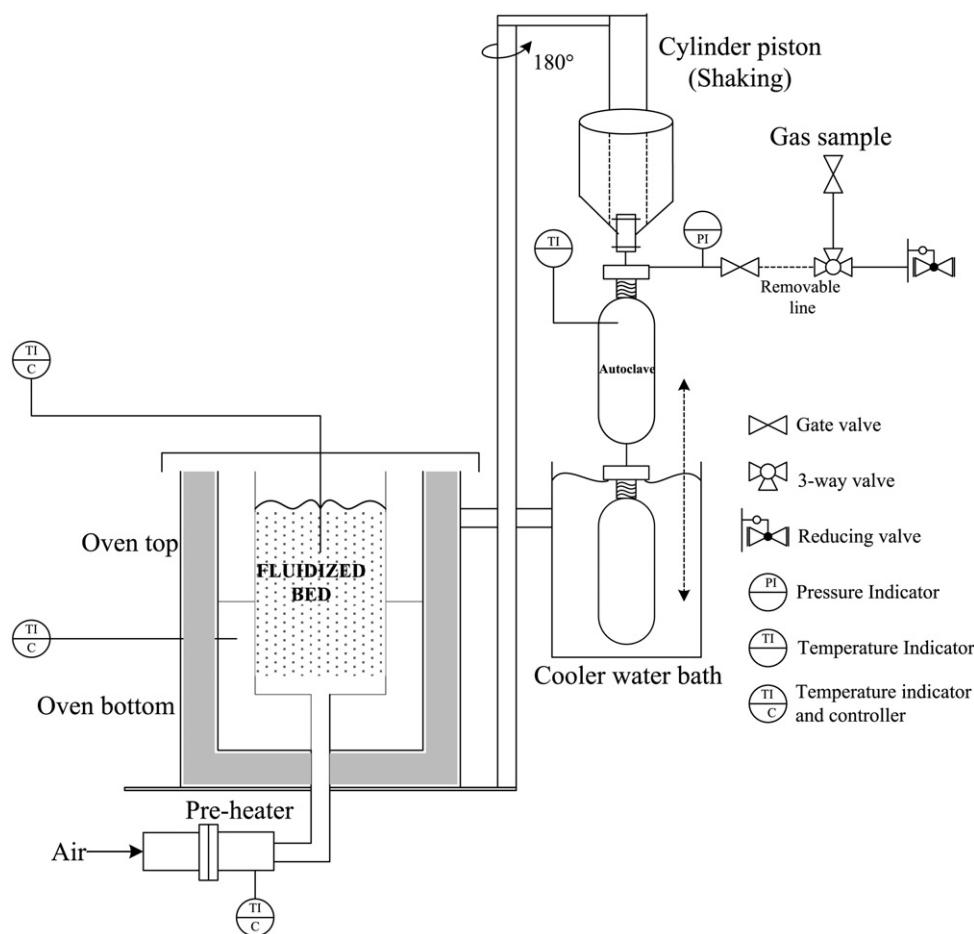


Fig. 1. Schematic diagram of the experimental batch autoclave reactor set-up.

yield, and where possible, to optimize/tune the product gas towards either H_2 or CH_4 rich gas.

The objective of this study is therefore to contribute to the understanding of the chemistry of biomass gasification in supercritical water by elucidating the relationship between molecular structures (chain length, functional groups) on the gasification behaviour. Carboxylic acids and alcohols are most frequently observed intermediate products from the hydrothermal gasification of a wide variety of organic compounds, wastes and biomass, and were therefore chosen for systematic study [6,7]. The goal of this work was to investigate experimentally if and how the chain length of linear alcohols and acids affects the product distribution during SCWG of these compounds. In this work the following series of experiments were carried out to study:

1. The influence of chain length of linear organic acids ranging from C_1 to C_8 compounds on the gasification behaviour in terms of product gas yields and carbon to gas conversion.
2. The influence of chain lengths of n-alcohols ranging from C_1 to C_8 on the gasification behaviour.
3. The effect of increasing number of $-OH$ groups and the positioning of these groups.

2. Experimental methods

2.1. Materials, experimental set-up and procedures

All chemicals used in this study were obtained from Sigma Aldrich with a high purity. The experiments were carried out in a batch autoclave reactor (Inconel alloy: $\sim 72\%$ Ni, 15% Cr and $\sim 8\%$ Fe)

having an internal volume of 45 mL and a schematic diagram of the set-up is shown in Fig. 1. For safety reasons, the reactor set-up was placed in a high pressure room and is controlled from outside the room during the experiments. The reactor is equipped with two orifices, one for a thermocouple and the other to connect to a pressure indicator and gate valve. The pressure and the temperature of the reactor is recorded and monitored using Pico Log software. With the help of a pneumatic arm, the autoclave can be immersed into and removed out of the fluidized sand bed after the reaction. This sand bed was heated by an electric oven (with preheated fluidization gas).

The experimental procedure is as follows: in a typical run, the calculated amount of aqueous feed solution is loaded into the reactor and screwed tightly and connected to the pneumatic arm of the set-up. The final reactor pressure reached is an outcome of the initial amount of water added to the reactor which is calculated based on the density of water at the experimental conditions to be investigated. The line with the pressure reader was connected to the autoclave and flushed with nitrogen several times to remove any oxygen present in the system. The reactor was then pressurized with 20 bar of nitrogen which served the purpose for leak test. The line connecting to the autoclave was removed and the high pressure room was closed and the remainder of the experiment was monitored from outside. Using the pneumatic arm, the autoclave is positioned on the fluidized sand bed and then the reaction was initiated by immersing the autoclave with the help of a piston into the preheated fluidized sand bed which had a temperature of $\sim 30^\circ C$ higher than the desired reaction temperature. All the experiments were carried out at $600^\circ C \pm 10$, 260 ± 30 bar and 15 min of reaction time. After the desired reaction

time, the reactor was lifted and quenched in a cold water bath.

Gas samples were taken in a syringe and analyzed with an off-line gas chromatography. With the gas composition, the final pressure and temperature inside the reactor, the amount of each gas produced was calculated. After the reactor was cooled, it was depressurized and the autoclave was disconnected from the arm and opened. The remaining product (liquid and solids in suspension) was then collected in a glass bottle and the reactor was rinsed with acetone to remove any water-insoluble deposits. The aqueous phase was analyzed for dissolved organic carbon with an elemental analyzer (Fisons Instruments 1108 EA CHN-S). Gas chromatography–mass spectrometry (GC–MS) analysis was performed with an Agilent GCMS 6890N to identify the intermediate compounds in the liquid effluent after the reaction. The carbon balance closure was found to be in the range of 97–99% for C₁ and C₂ alcohols and acids. However, for higher chain lengths of carbon containing alcohols and acids the carbon balance is not close to 100% due to the formation of char/tar formation.

2.2. Terms and definitions

The gasification efficiency (GE) or carbon to gas conversion is defined as the degree of conversion of carbon in the feed to “C” containing gases.

$$\text{(Carbon) gasification efficiency, } C_{\text{.GE}}(\%) = \frac{\sum_i N_{\text{C},i}}{N_{\text{C,feed}}} \times 100$$

$$\text{Hydrogen gasification efficiency, } H_{\text{.GE}}(\%) = \frac{\sum_i N_{\text{H},i}}{N_{\text{H,feed}}} \times 100$$

$$\text{Oxygen gasification efficiency, } O_{\text{.GE}}(\%) = \frac{\sum_i N_{\text{O},i}}{N_{\text{O,feed}}} \times 100$$

The yield (Y_i) of product gas is defined relative to the carbon content by:

$$Y_i = \frac{N_{\text{C},i}}{N_{\text{C,feed}}}$$

where $N_{\text{C,feed}}$, $N_{\text{H,feed}}$, $N_{\text{O,feed}}$ are the number of moles of carbon, hydrogen and oxygen in the feed. Whereas $N_{\text{C},i}$, $N_{\text{H},i}$ and $N_{\text{O},i}$ are the number of moles of carbon, hydrogen and oxygen atoms, respectively, in product gas ($i = \text{CO}, \text{CO}_2, \text{CH}_4, \text{C}_2\text{H}_4, \text{C}_2\text{H}_6, \text{C}_3\text{H}_6, \text{C}_3\text{H}_8$).

3. Results and discussion

Series of experiments are carried out to determine the influence of increasing the chain length of organic acids and alcohols, the number of OH groups and the positioning of OH groups on the gasification behaviour in SCW.

The postulated reaction pathways, under the assumption of radical reactions being dominant, for the decomposition of acids and alcohols in SCW are based on our experimental observations and from literature studies. As the complexity increases for higher chain lengths of carbon atoms, only for acids and alcohols with one, two and three carbon atoms the reaction schemes are presented and focus on the formation of permanent (product-) gases from these oxygenated model compounds.

The mechanisms proposed are formulated, on basis of a competitive scheme for the three parallel base-type reactions; being C–O, C–H and O–H bond scission. For higher carbon chain atoms, additionally the C–C bond breaking is taken into consideration. This competition of bond scissioning dictates the product distribution. It is tried to identify on basis of experimentally determined product

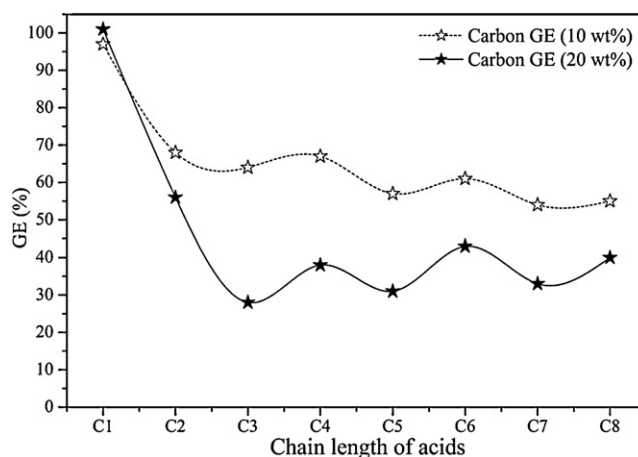


Fig. 2. The carbon to gas conversion of different chain lengths of organic acids.

distributions obtained in this work to derive from this preferred, or dominating, reaction paths.

3.1. Gasification of organic acids

We studied the influence of different chain lengths of organic acids and alcohols ranging from C₁ to C₈ on the gasification behaviour in supercritical water.

Fig. 2 illustrates the trend in the carbon to gas conversion for two different concentrations (10 and 20 wt%) of a homologous series of linear organic acids, having carbon chain lengths from C₁ (formic acid) to C₈ (octanoic acid). It is evident from Figs. 2 and 3 that among all the acids, formic acid decomposes completely and rapidly into gases. The carbon GE decreases initially rapidly with increasing chain length after formic acid, but more slowly from C₃ onwards. The gasification efficiency trend shows a remarkable, damped oscillatory behaviour. Organic acids with an even number of carbon atoms were found to have higher GE than those with an odd number of carbon atoms in the hydrocarbon chain. This trend is persistent, even for higher organic acids, and is visible for both the 10 wt% and the 20 wt% series. The initial feed concentration has a significant impact on the carbon GE. This is possibly due to polymerization reactions occurring during the initial phase of the reaction leading to enhanced polymerization and subsequent tar and char forming reactions with at high feed concentration. A polymerization has a higher reaction order than degradation; therefore it is always favoured at higher concentrations [8]. Visual observations of the reactor after the experiments reveal/confirm some char and tar formation with higher acids (after C₂).

The dry gas composition and product gas yields with increasing carbon chain length of organic acids with concentrations of 10 and 20 wt% are shown in Fig. 3a and b, respectively. It is clear from Fig. 3a that there is hardly any influence of the initial feed concentration on the dry gas composition which suggests that the gas formation mechanism remains unaltered with initial feed concentration (Fig. 3a). This is in accordance with the assumption that the polymerization is a competitive parallel reaction [8]. The trends of product gas yields (mol/mol) are similar for both 10 and 20 wt% concentration. Higher gas yields are obtained for the less concentrated feed stocks, as expected from the gasification efficiency results discussed earlier (Fig. 3b).

3.1.1. Formic acid

Formic acid is an often reported intermediate product in the hydrothermal oxidation of a wide variety of organic compounds and wastes. The smallest of all carboxylic acids decomposes rapidly in SCW via two parallel paths, decarboxylation (forming CO₂ and

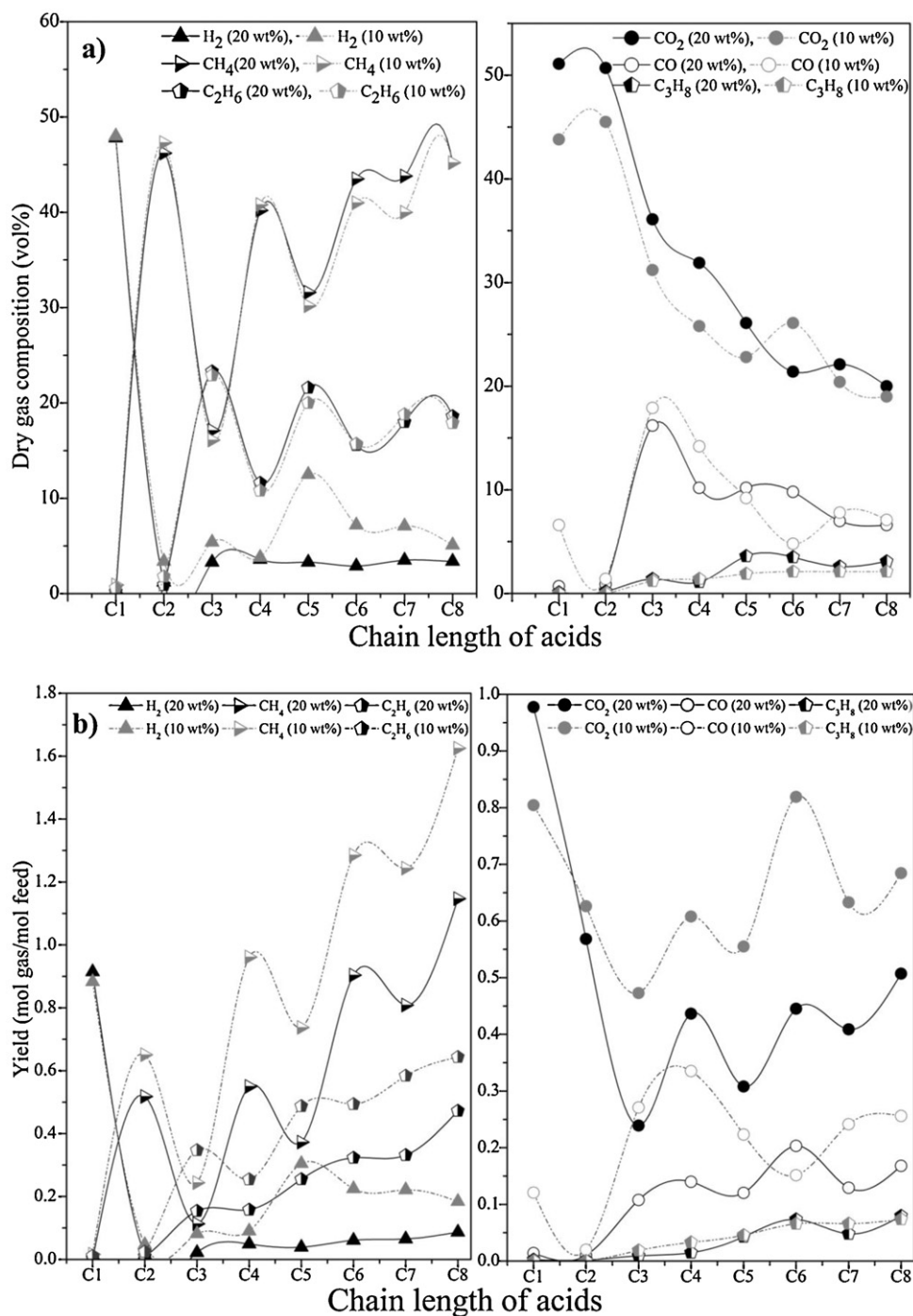


Fig. 3. The influence of different chain lengths of organic acids on (a) dry gas composition (vol.%) and (b) product gas yields (mol/mol) (dark and thick symbols corresponds to 20 wt% organic concentration, light and dotted trend lines represent 10 wt% organic concentration).

H₂) and dehydration (into CO and H₂O) [9–12]. The postulated free-radical mechanism for the formic acid decomposition in SCW is shown in Fig. 5.

This free radical mechanism is discussed here because of the rather high temperature and low density (70.8 kg m⁻³) in the experiments discussed here. High temperature and low densities should promote free radical reactions [13]. In addition this mechanism is used as basis for the free-radical mechanism used for the higher carboxylic acids. On the other hand a molecular mechanisms catalyzed by water has to be considered, explaining the preference of decarboxylation at neutral conditions [9,14,15].

Routes 1, 4 and 11 are initiation reactions for the free radical chain mechanism. By this reaction, but mainly via the reactions with free-radical inside the chain, the bond breaking of O–H, C–H, and C–O occurs. Water is able to serve as transfer medium: free radicals reacting with water leads also to H[•] and OH[•] free radicals taking part in the chain. For this no influence on the chemical reaction rates is found [16]. On the other hand the solvent nature of supercritical water seems to have a significant influence, also in the free-radical mechanism [17,18]. Routes 1 and 4 are thermolytic scissioning of a bond, releasing H[•]. Routes 2 and 5 are induced by OH[•], while Route 3, 6 and 10 are initiated by H[•]

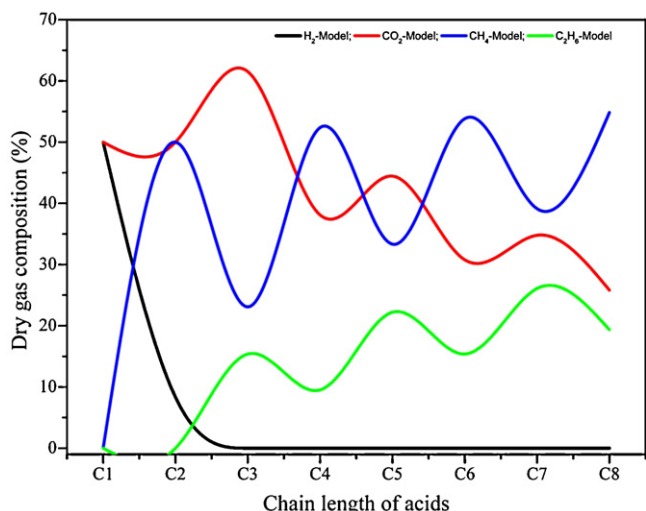


Fig. 4. Model predictions of dry gas composition of different chain lengths of organic acids.

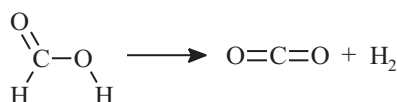
radicals. In principle also other, carbon-containing free radicals, not only OH^\bullet and H^\bullet , would lead to the same products. But these would not lead to new and independent reaction pathways, because the reactions of carbon containing free radicals are already considered. Routes 1–3 are abstraction of acidic hydrogen at the oxygen atom, leading to the formation of HCOO^\bullet radicals which are stabilized by resonance effects (delocalization of electron). The HCOO^\bullet radicals further decomposes into CO_2 and releases one H^\bullet (Route 8). Route 4–6 are the abstraction of hydrogen at α -carbon atom that leads to formation of $\text{OC}^\bullet\text{OH}$ radical which further decomposes into CO_2 and releases one H^\bullet (Route 9). Route 10, is a dehydration route where H^\bullet reacts with OH group present in the compound and forms water and CO and releases one H^\bullet . CO can be further converted into CO_2 via the WGS reaction.

In the mechanism shown here, e.g., in Fig. 5, the WGS reaction is shown as a free radical reaction. As mentioned above, a molecular mechanism via formic acid is also discussed. In this

case the activation energies for the two pathways, to CO and to CO_2 , are nearly identical without water and the formation of CO_2 is preferred in the case of complex formation with water. Still in this case the difference is only around 31 kJ/mol [14]. In the case not CO is formed but formic acid, small differences in the reaction medium would change the preference to CO or CO_2 . It is therefore not surprising that sometimes the preferred product determined changes with reaction conditions: Wakai et al. [19] studied the decomposition of formic acid (0.1 to 1 M) at temperatures between 275 °C and 350 °C in quartz tubes. The carbon-containing products were measured by NMR after around 10 min reaction time. At low concentration and 300 °C CO_2 was the main product. At higher concentration CO was the dominant product. This was explained by an autocatalytic effect. For the 1 M solution, CO was the main product in the whole temperature range and the CO concentration was only slightly decreasing with temperature. The addition of metal powder (SUS 316L, Hastelloy C-276, Inconel 625; all common high-pressure vessel materials) supports decarboxylation.

Singleton et al. [20] in their experiments at low temperature found that the dominant interaction of the OH^\bullet radicals is with the acidic hydrogen of formic acid, rather than with the formyl hydrogen. Although at high temperatures, abstraction from the formyl hydrogen would be expected to make a significant contribution because of its anticipated positive activation energy [20]. Hence, reactions 1–3 seem to be the major reaction pathways.

The overall reaction (decarboxylation) can be written as:



Although dehydration (reactions 10, 11) may occur to some extent, the above (decarboxylation) is therefore expected to be the major reaction pathway.

The experimental obtained gas composition, 51% CO_2 and 48% H_2 , confirms that decarboxylation is dominant over dehydration. It could be argued that the dehydration reaction initially might have taken place, forming CO which further oxidizes into CO_2 via WGS reaction. Marginal amount (0.74%) of CO present in gas phase, indicates, however, a low extent of the dehydration reaction, as otherwise CO should have been present in significant amounts as seen in our gasification experiments using alcohols (discussed next section). It is very unlikely to convert CO to such a large extent (near to equilibrium) without the presence of any catalyst. The high CO_2 selectivity obtained is in-line with literature [9]. Remarkably, studies of formic acid decomposition in the gas phase was dehydration, which forms CO and H_2O , and that decarboxylation, which forms CO_2 and H_2 , occurred to a lesser extent. However, based on literature [9,14,15] and our experimental results above indicate that the main reaction under hydrothermal conditions is decarboxylation and that dehydration is insignificant.

3.1.2. Acetic acid

Acetic acid is one of the stable intermediate products that are often found during the degradation of several biomass wastes and it is proven to be quite refractory in SCWG [1,4,6,7]. A postulated mechanism for acetic acid decomposition, again based on a radical reaction mechanism, is shown in Fig. 6. Considering the gas phase composition found (46% CH_4 and 51% CO_2) it can be seen that the more significant reaction pathway is hydrogen abstraction from the carboxyl group (OH bond scission, path 1), as this leads to equimolar formation of CO_2 and CH_4 .

According to Meyer et al. [21] acetic acid does not decompose up to temperatures of 400 °C and it starts to decompose into methane

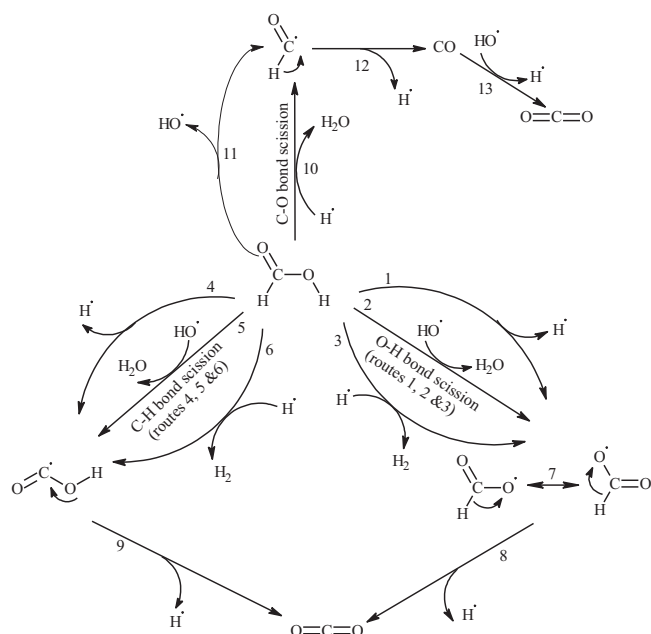


Fig. 5. Postulated reaction mechanism of formic acid decomposition in SCWG (reactions are indicated with numbers).

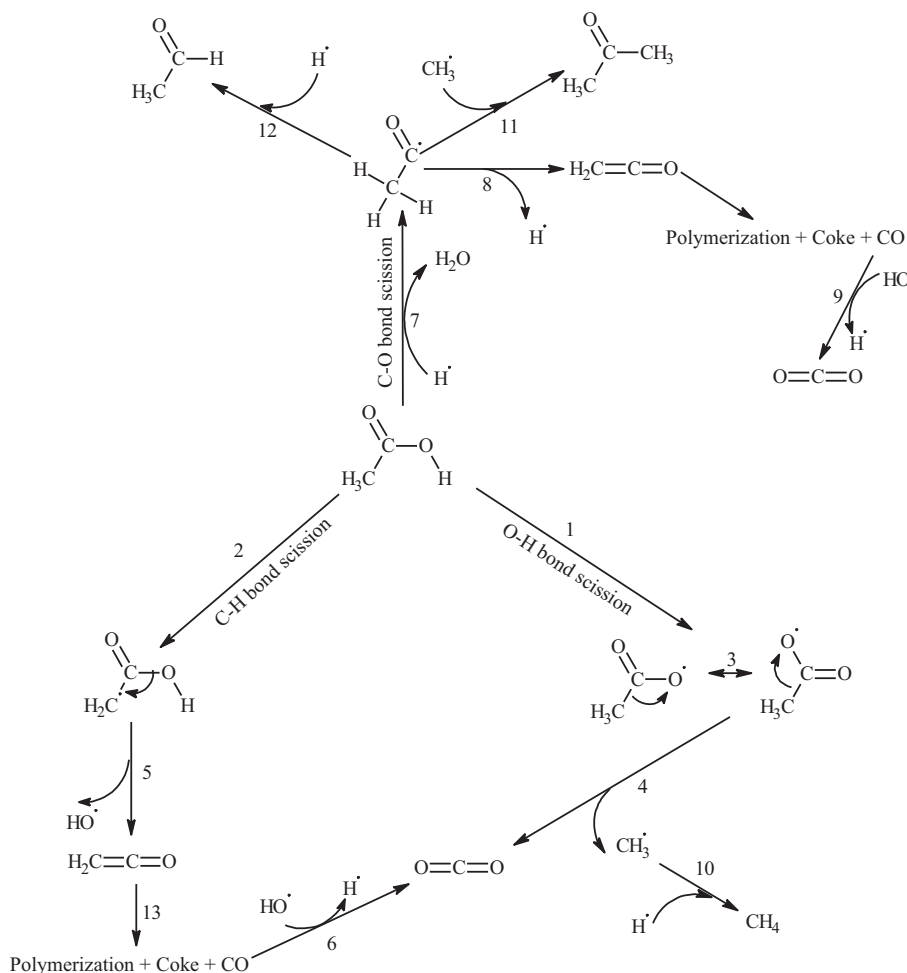
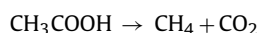


Fig. 6. Postulated reaction mechanism of acetic acid decomposition in SCW (to keep the scheme simpler, C–H and O–H bond scission reactions are just indicated and the reaction pathways are analogous to those shown in Fig. 5).

and carbon dioxide at above 450 °C. Watanabe et al. [22,23], found that acetic acid was very stable in the absence of any additive at 400 °C after 1 h of reaction time. They proposed two reaction schemes, monomolecular decarboxylation (CH_4 and CO_2) with the addition of KOH and bimolecular decarboxylation (acetone and CO_2) in the presence of ZrO_2 .

The dissociation energies of different bonds present in acetic acid are as follows: $D(\text{CH}_3\text{COO}-\text{H}) = 105.8 \pm 2$ kcal/mol, $D(\text{H}-\text{CH}_2\text{COOH}) = 98 \pm 2$ kcal/mol (assumed to be the same as $D(\text{H}-\text{CH}_2\text{COCH}_3)$) [24]. Although $D(\text{CH}_3\text{COO}-\text{H}) > D(\text{H}-\text{CH}_2\text{COOH})$, the experimental data show that the O–H bond is more likely to break. In case of breaking of C–H bond breaking in $\text{H}-\text{CH}_2\text{COOH}$ (path 2 (and 4–6 in Fig. 5)), a ketene (CH_2CO) is formed (via dehydration). Generally, ketenes are very reactive and convert into polymeric compounds and gases: coke (carbon), resin, CO , CO_2 [25]. However, no large fraction of coke was formed.

The overall reaction scheme for acetic acid considering $\text{COO}-\text{H}$ bond breaking is:



The GC–MS analysis of the liquid samples indicated the presence of acetic acid in significant amounts. A minor amount of acetone is also detected in the liquid phase, for which the formation route is also shown in the proposed mechanism (Fig. 6). The dominating pathway, however, proceeds via an O–H bond scission, resulting in the formation of equimolar amounts of CO_2 and CH_4 (Fig. 3).

3.1.3. Propionic acid and other high molecular weight acids

For propionic acid decomposition a proposed mechanism is shown in Fig. 7. The GC–MS analysis of the liquid phase product after the reaction identified propionic acid and acetone as main components (next to water) in the liquid phase. Very small amounts of acetic acid were detected in the liquid phase, indicating that breaking of C–C bond (pathway 16 followed by 17) now also occurs as initial step. Once acetic acid forms, it can produce acetone, CO_2 and water via bimolecular decarboxylation [26]. Small amount of benzene is also present in the liquid, pointing to the occurrence of aromatization reactions, leading to the formation of very stable aromatic compounds.

From the GC–MS analysis the major compound found in the liquid phase after the reaction was, however, the unconverted acid itself (>95% of the organic compounds in the aqueous phase). Acetic acid was the major refractory compound that was identified in all the acid cases (except for formic acid decomposition), indicating the scissioning of C–C bonds leading to the formation of lower acids, which will then further undergo C–C cracking till acetic acid forms.

Acetic acid may convert into acetone by bimolecular decarboxylation [26]. Acetic acid and acetone are the most stable compounds. For lower acids, up to C_4 , acetic acid was present in small amounts while for higher acids, acetic acid was the most abundant compound in the liquid phase. That is in-line with concept that higher hydrocarbons are easier to crack [27]. Benzene and toluene were found in small amounts when gasifying higher acids, indicating that aromatization reactions are also taking place. For higher acids we

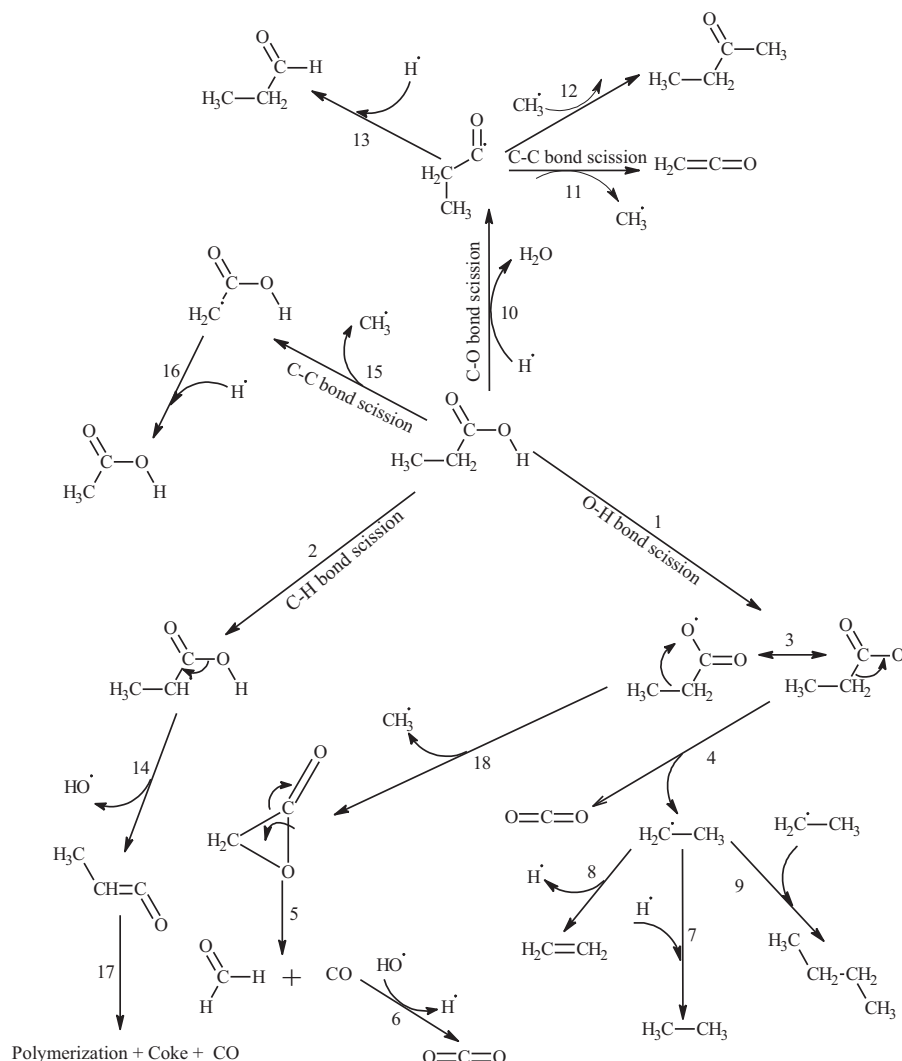


Fig. 7. Postulated reaction mechanism of propionic acid decomposition in SCW (to keep the reaction scheme simpler, C–H and O–H bond scission reactions are just indicated and the reaction pathways are analogous to those shown in Fig. 5).

suspect that abstraction of α -hydrogen becomes significant, leading to the formation of ketene. Jin et al. have studied the oxidation reactions of high molecular weight carboxylic acid (stearic acid) in SCW and they proposed the reaction of high molecular weight carboxylic acids in SCW proceeds with the consecutive oxidation of higher molecular weight carboxylic acids to lower molecular weight carboxylic acids through several major pathways [28].

3.1.4. Modelling approach

Overall, it is found that the gasification of linear carboxylic acids in supercritical water starts predominantly with the scissioning of the O–H bond of the acid group. Subsequently, β scissioning is dominating in fractionation and gas formation, as argued below.

With this simple approach, the characteristic oscillatory behaviour of the gas product distribution with increasing alkyl chain length, as observed in Fig. 3a, can be explained. In case of an even numbered carbon organic acids, initial acidic O–H bond scission followed by β scission leads to formation of CO_2 and a $(n - 1)$; hence odd number) alkyl radical. Continued β scission leads to significant C_2 formation and ends by the formation of a CH_4 molecule (from CH_3 radical). For an odd numbered carboxylic acid, this process does not lead to the formation of a final CH_4 molecule.

Exact this oscillatory behaviour of the gas composition trend is seen in Fig. 3, where more CH_4 and less C_2H_6 have been found

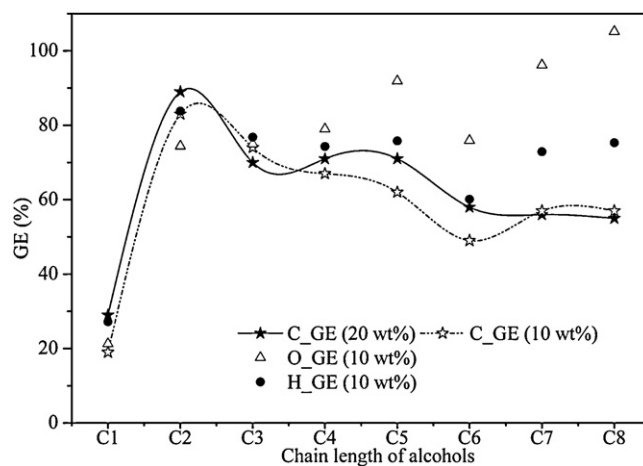


Fig. 8. The gasification efficiencies of different chain lengths of alcohols (carbon GE was shown for 20 and 10 wt% feed concentration while the oxygen and hydrogen GE was shown for 10 wt% concentration).

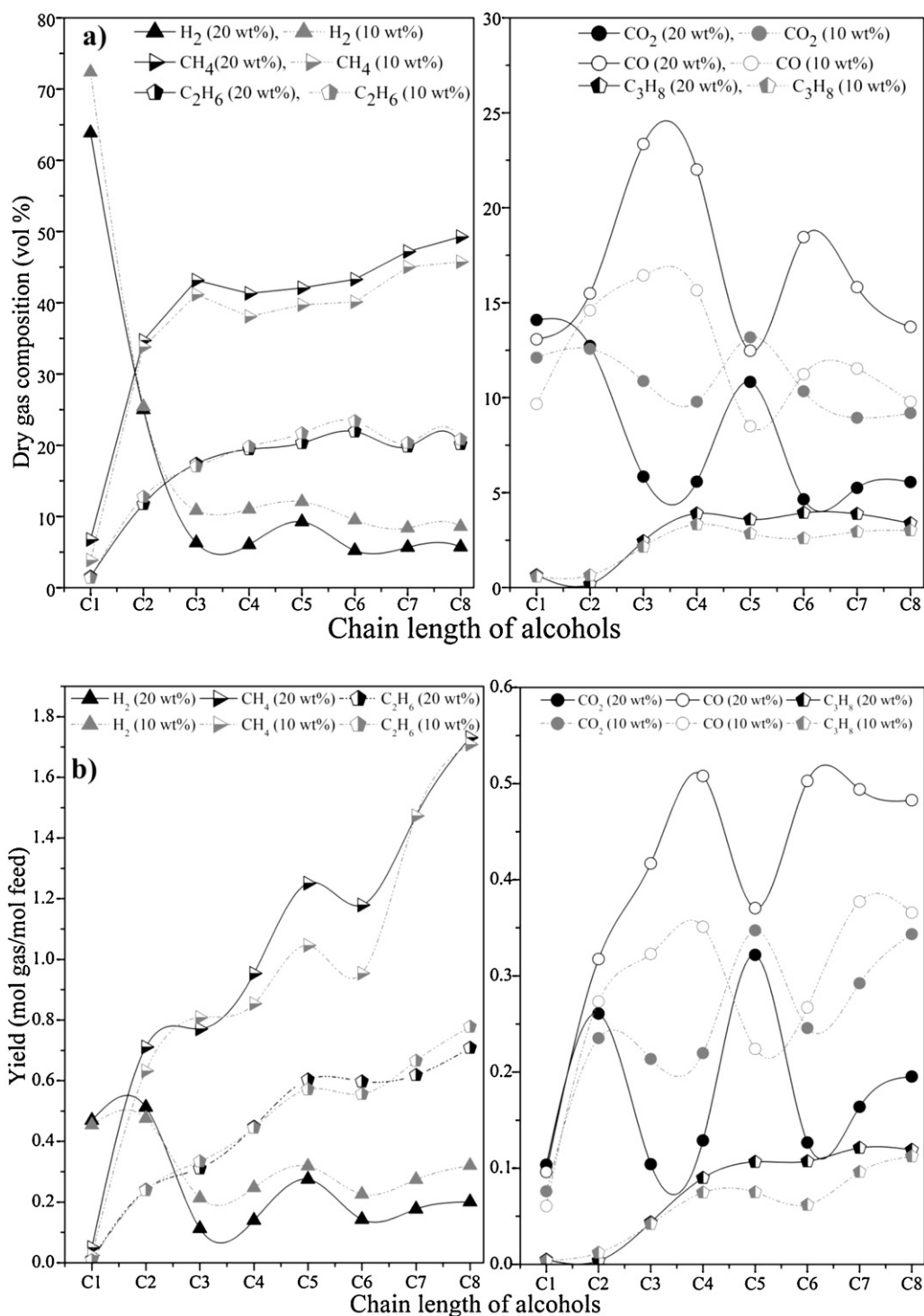


Fig. 9. The influence of different chain lengths of organic alcohols on (a) dry gas composition (vol.%) and (b) product gas yields (mol/mol) [dark and thick symbols corresponds to 20 wt% organic concentration, light and dotted trend lines represent 10 wt% organic concentration].

in case of even numbered carbon organic acids. The oscillatory behaviour is super-positioned to another general trend that with increasing chain length more CH₄ is formed (Fig. 3b), most likely due to the increasing number of possible reactions and interactions between intermediates and apparently also resulting in more CH₄.

The oscillations in the GE trend (Fig. 2) cannot be explained by this, but may be caused by constraints in the chemical analysis. When, e.g., C₂H₅ radicals recombine with other alkyl radicals this leads to the formation of alkanes larger than butane which were

not detectable by the installed GC. This may be the reason of our GE trend in which, in case of even numbered carbon acid GE is higher than for odd numbered carboxylic acids.

A simple model was developed to estimate the product gas distribution of different chain lengths of organic acids. Fig. 4 is the model predictions of product gas distribution from different chain lengths of organic acids. Two assumptions were made for the model development that is complete conversion of acids to product gases and 75% conversion of C₂ compounds that is initially formed via

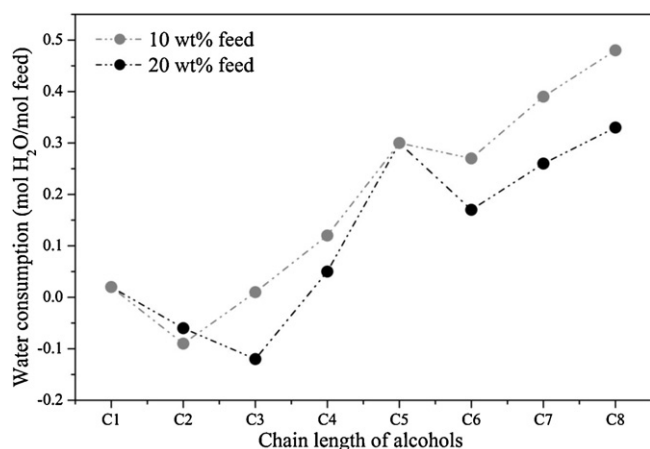
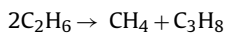


Fig. 10. The extent of water consumption for different chain lengths of alcohols.

β -scission as described earlier to methane formation according to the following reaction given below.



It is evident that the oscillatory behaviour of alkanes (CH_4 and C_2H_6) and the decreasing trend of H_2 and CO_2 from the experiments shown in Fig. 3a are very well in line with the model trends presented in Fig. 4.

3.2. Gasification of alcohols

In this section results for a study on the influence of the alkyl chain lengths of linear n-alcohols ranging from C_1 to C_8 on the gasification behaviour in supercritical water will be reported.

The carbon GE trend for alcohols of different chain lengths, using 10 and 20 wt% solutions, is shown in Fig. 8. It is evident from the figure that methanol has the lowest GE and ethanol the highest. After ethanol, a slight decrease in GE with increasing chain length is noticed. This can be attributed to the formation of intermediate compounds and their polymerization reactions leading to the formation of tar and char eventually reducing the GE. The alcohol concentration itself was found to have a minimal impact on the carbon GE, see Fig. 8. This is in contrast with earlier findings for the gasification efficiency for organic acids of different chain lengths; see Fig. 2 for comparison, where the concentration effect is significant.

The product gas composition (vol.%) and yields (mol/mol) for different chain lengths of alcohols are shown in Fig. 9a and b, respectively. From Fig. 9a, major differences in the gas composition is noticed until the C_3 compound and after C_3 (1-propanol), the dry gas composition does not change much with increasing chain length, except for carbon distribution over CO and CO_2 . The dry gas composition on gasification of alcohols with increasing alkyl chain length shows opposite trends for CO and CO_2 , for which no explanation was found. The sum ($CO + CO_2$) is, however, consistent and in line with the carbon to gas conversion and also the oxygen balance (see Fig. 8) shows a monotonous trend with chain length, despite the large variations in CO and CO_2 fraction.

The difference between the total moles of oxygen atoms in the ($CO + CO_2$) formed and the moles of gasified (parent) organic alcohols will give an estimation of the moles of oxygen atoms that must have transferred to or from water.

The oxygen and hydrogen gasification efficiencies for 10 wt% feed concentrations are higher than the carbon gasification efficiency after C_2 compounds (Fig. 8). From the oxygen-atom balance, the number of moles of oxygen atoms released equals the moles of organics gasified. A large fraction of that oxygen is recovered in the

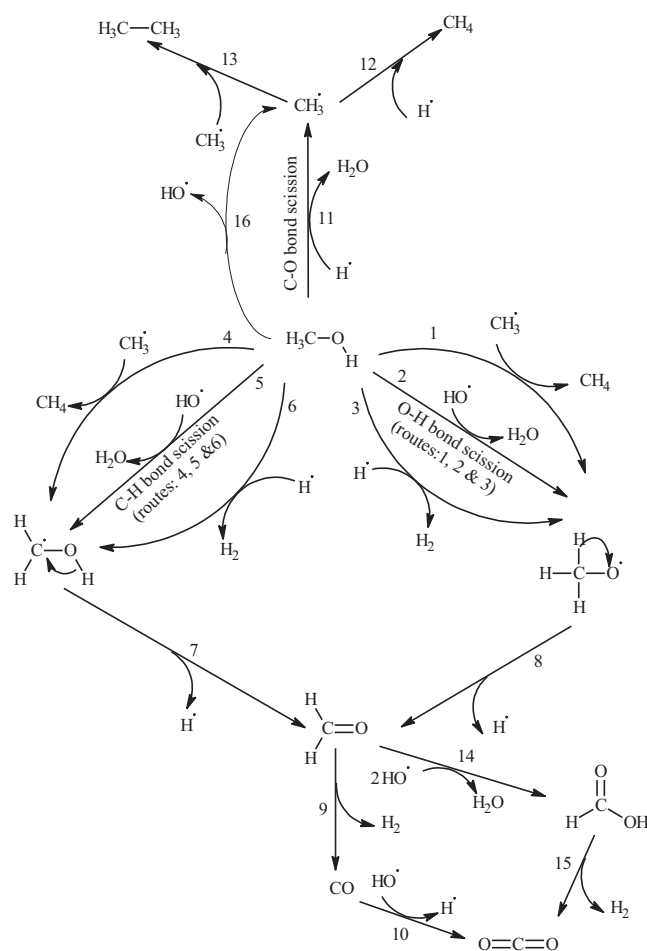


Fig. 11. Postulated reaction mechanism of methanol decomposition in SCW (reactions are indicated with numbers).

gas phase in the form of CO and CO_2 and the rest will be used to produce water via dehydration reaction. The opposite, more oxygen atoms in the gaseous products than released by the gasification of the organic molecules ('oxygen excess') is also possible. In that case, oxygen is obtained from the water phase and used to form CO_2 and additional hydrogen.

From the increase in the gap between CO and CO_2 with increasing organics concentration (Fig. 9a and b), it is suggested that this may have a large influence on the WGS reaction, as the water concentration is decreasing when going from the 10 wt% to 20 wt% series.

The calculated oxygen-based GE was found to be higher than the carbon-based GE from C_4 to C_8 alcohols, suggesting the participation of water in the reaction. The number of moles of water consumed per mole of organics with increasing chain length for the alcohols studied can be appreciated from Fig. 10. This implies that with increasing chain length the extent of dehydration reaction decreases, indicating that C–OH bond becomes relatively more difficult to scission in comparison to the other bonds and C–C bond cracking becomes dominant as we increase the chain length; which is in line with findings for thermal cracking of hydrocarbons [24,29]. Dehydration reactions become negligible after butanol and there is no significant influence of concentration on the extent of dehydration reaction.

3.2.1. Methanol

In the absence of any catalyst and at temperatures below $600^\circ C$ in SCW, methanol is confirmed in this work to be a stable

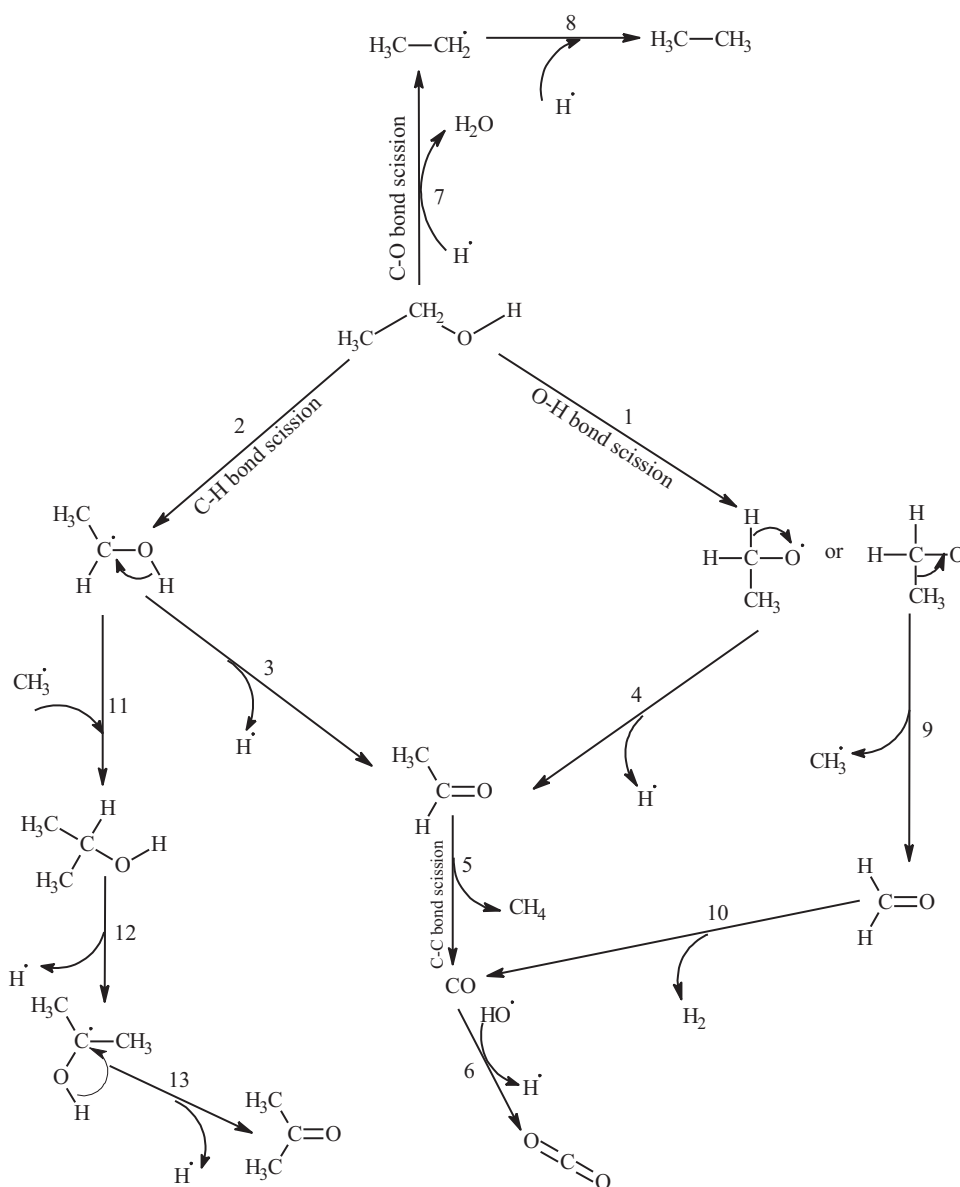


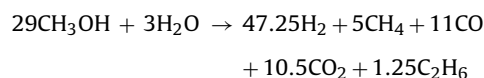
Fig. 12. Postulated reaction mechanism of ethanol decomposition in SCW (to keep the reaction scheme simpler, C–H and O–H bond scission reactions are just indicated and the reaction pathways are analogous to those shown in Fig. 11).

compound [30]. The activation energies for pure methanol are reported as high as 191 kJ/mol, whereas the activation energy for ethanol was reported to be 145 kJ/mol [31,32].

A postulated mechanism for the methanol decomposition based on the experimental results and literature [22,31–34] in SCW is shown in Fig. 11. Routes 1–3 are the abstraction of acidic hydrogen at oxygen atom that leads to formation of $\text{H}_3\text{CO}^\bullet$ radical which decomposes into formaldehyde and releases one H^\bullet (Route 8). The formaldehyde that is formed can either decompose directly into CO and H_2 (Route 9) or it can oxidize into formic acid which then further decompose to CO_2 and H_2 . An alternative initiation reaction is the abstraction of the hydrogen at the α -carbon atom (reactions 4–6), which may again lead to formaldehyde (Route 7). The scission of the C–O bond, Route 11, is the dehydration route in which a H^\bullet radical reacts with an OH group present in the compound and forms water and CH_3^\bullet , which will lead to methane formation. The methyl radical can further take part in many other routes, as shown in Fig. 10. Considering the gas composition it can only be concluded that C–O bond breaking, leading to CH_4 formation, is the

least favoured initiation pathway, since the CH_4 yield was found to be very low. The two other reaction pathways, C–H and O–H bond breaking, lead to a similar product composition ($\text{CO} + 2\text{H}_2$).

The overall reaction stoichiometric for 20 wt% methanol concentration, as based on the experimental gas yields and methanol to gas conversion, can be written as:



Traces of formic acid and formaldehyde were reported to be present in the effluent liquid of methanol decomposition in SCW [31,33] using HPLC analysis and were also found in this study.

The relative low GE of methanol (Fig. 8) in a metal reactor compared to other studies [35] shows that the catalysis of the reactor wall is of minor importance here. Possible explanation is the relative low surface-to-volume ratio and perhaps passivation reducing the catalytic effect.

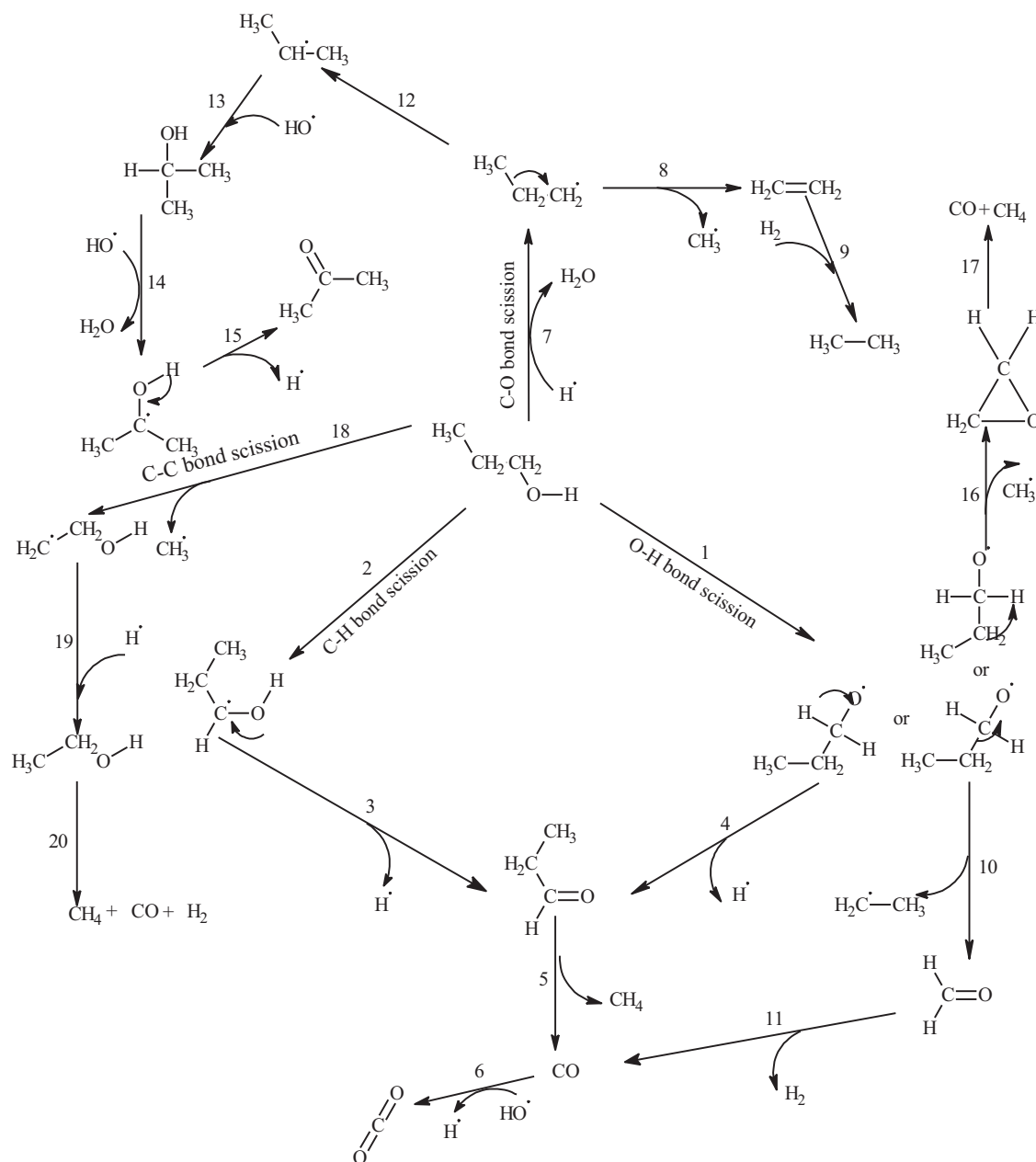


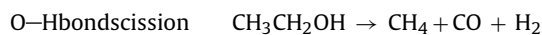
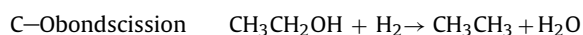
Fig. 13. Postulated reaction mechanism of 1-propanol decomposition in SCW (to keep the reaction scheme simpler, C–H and O–H bond scission reactions are just indicated and the reaction pathways are analogous to those shown in Fig. 11).

3.2.2. Ethanol

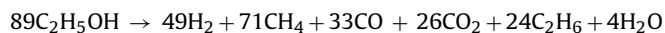
A postulated mechanism for the ethanol decomposition in SCW is shown in Fig. 12. Considering the experimentally found gas composition it can be seen that all the three routes, C–O bond breaking, C–H, hydrogen abstraction and O–H, hydrogen abstraction are competing each other. Unlike the case of methanol where C–O bond cleavage was least favourable, here the presence of C_2H_6 in significant amounts indicates that C–O bond cleavage is also a significant reaction pathway. According to the scheme in Fig. 10, the initiation by O–H bond scission and followed by C–C scission should result in around 50% carbon selectivity towards CH_4 . The dry gas composition in Fig. 9b confirms therefore that this pathway is likely to dominate.

GC–MS analysis of the liquid phase showed that ethanol is the only significant product present in the liquid phase. Writing the

reaction pathways for ethanol gasification in SCW in simple overall equations:



The overall reaction considering the experimental gas yields of 20 wt% ethanol to gas conversion can be written as:



Arita et al. [36] have reported the conversion of ethanol to hydrogen in supercritical water at 450–500 °C in a quartz reactor and proposed two reaction schemes, based on dehydrogenation and dehydration. Ethanol dehydrogenation was the major pathway that

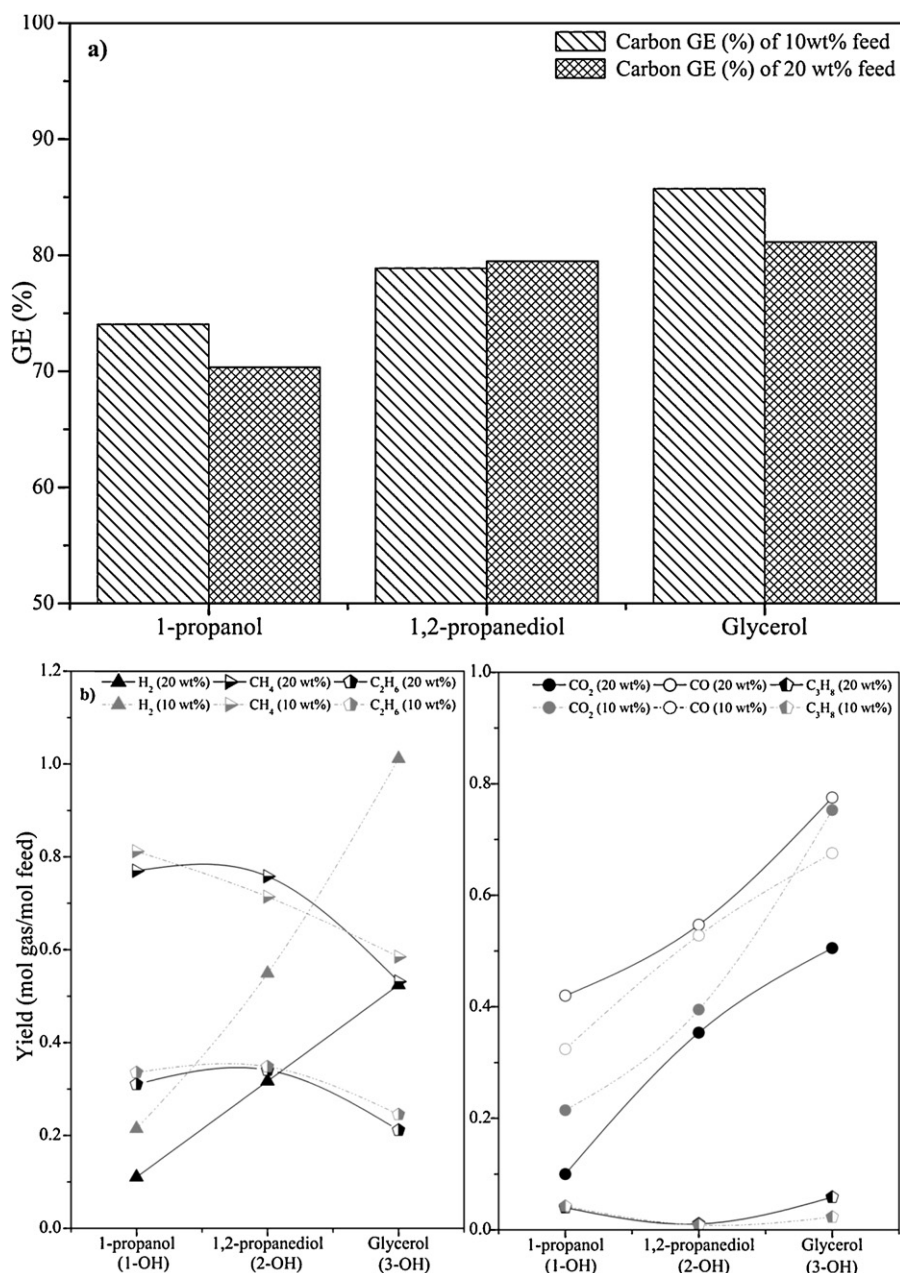


Fig. 14. Influence of the number of OH groups on the gasification behaviour: (a) carbon to gas conversion and (b) product gas yields (symbols with thick trend lines corresponds to 20 wt% organic concentration, symbols with dotted trend lines represent 10 wt% organic concentration).

leads to acetaldehyde, which further decomposes to CH₄ and CO, which is in-line with our proposed scheme shown in Fig. 12. The CO formed reacts via WGS to CO₂ and produces H₂. Acetaldehyde and trace amounts of methanol were detected in the effluent liquid of ethanol reforming in SCW [37].

3.2.3. 1-Propanol and higher alcohols

A similar radical reaction mechanism is postulated for 1-propanol and is shown in Fig. 13. It can be noticed that the schemes are rapidly gaining complexity going from methanol to ethanol to 1-propanol. The GC-MS analysis of the liquid phase after reaction showed the presence of significant amounts of unconverted 1-propanol in the liquid phase (as dominant compound). Small amounts of benzene and toluene are also detected in liquid phase, indicative for the occurrence of aromatization reactions. The GC-MS analysis of liquid phase products for other, higher alcohols (here: 1-butanol, 1-pentanol, 1-hexanol, 1-heptanol and

1-octanol) showed predominantly the presence of unconverted alcohols and some acetone and only very minor amounts of aromatic compounds derived from aromatization reactions. Kruse et al. [4] have studied the conversion of different C₄ compounds (1-butanol, 1-butanal, cis-butene-diol) in a batch reactor at 500 °C, 300 bar for 1 h and also reported the formation of these aromatic compounds (e.g., phenol, benzene, toluene, alkylbenzenes, alkylphenols, phenylethanones) for each of the C₄ compounds studied.

3.3. Influence of OH groups on gasification

3.3.1. Number of OH groups

Additionally we studied the influence of the number of OH groups and their position within the molecule on the product gas composition and gasification yield. To study the influence of number of OH groups, we chose 1-propanol, 1, 2-propanediol and

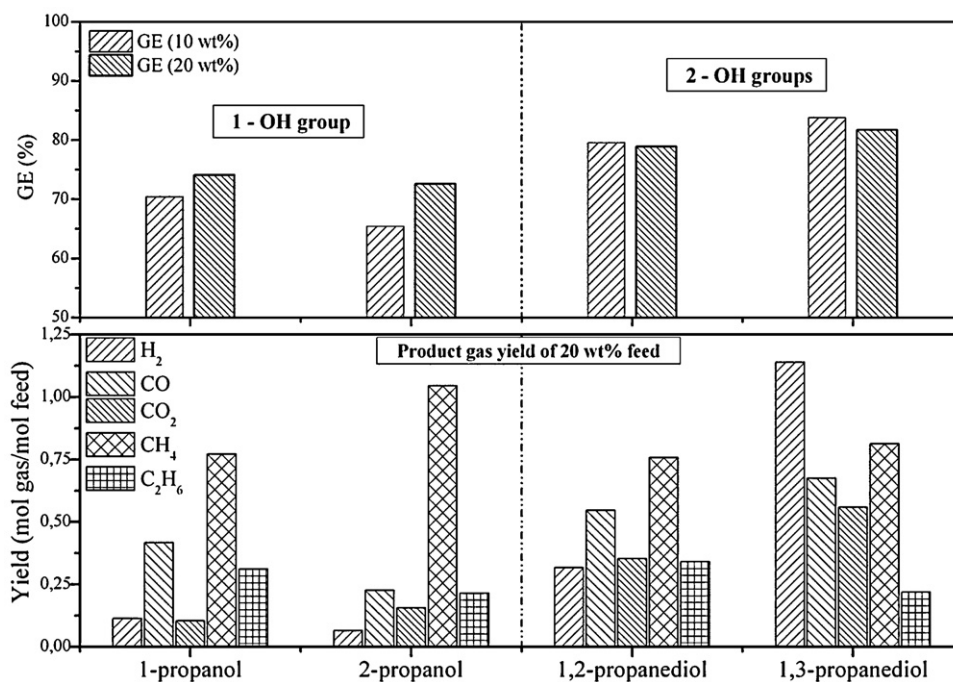


Fig. 15. Effect of the positioning of OH group at different locations on the GE and product gas yields.

glycerol containing one, two and three OH groups, respectively, as model compounds.

To study the influence of positioning of the OH groups, we chose 1-propanol and 2-propanol having one OH group at different locations. Another set of compounds used was 1, 2-propanediol and 1, 3-propanediol having two OH groups located at different positions.

The influence of number of OH groups on the GE and gas yields is shown in Fig. 14a and b, respectively. The initial feed concentration was found to have a minimal impact on the GE, which is in line with the results of alcohols as discussed earlier. From Fig. 14a it is clear that the GE increases slightly with the number of OH groups in the compound. The number of hydroxyl groups in the alcohols also significantly affected the product gas yields which is evident from Fig. 14b. With increasing number of OH groups, the combined yield of CO and CO₂ increases about proportional, whereas the hydrogen yield increases clearly more than proportional. This latter effect may be related to an increased WGS activity, or an altered decomposition mechanism. The yield of alkanes decreases with an increase in the number of OH groups as more oxygen atoms are present in the reactant molecule and an increase in the number of sites that can be attacked by hydroxyl radicals with increase in number of OH groups. Additionally, an OH group stabilizes the intermediate radicals formed by its electron-releasing nature, easing the gasification process. As the number of OH groups increases, the intermediates that are formed become more and more stable.

3.3.2. Positioning of the OH groups

The influence of the positioning of OH groups at different locations in the molecular structure is studied with 1-propanol and 2-propanol, both having one OH group, and 1, 2-propanediol, 1, 3-propanediol, both having two OH groups, on the gasification efficiency and product gas yield is shown in Fig. 15. It is clear from the figure that the CH₄ yield is higher and less C₂H₆ is formed with 2-propanol than in case of 1-propanol. Again, these results can be explained assuming that β -scission is a significant (dominating) reaction pathway in the formation of gases. In case of 2-propanol, β -scission leads to mainly methane and CO, while in case of

1-propanol, β -scission leads to the formation of methane, ethane and CO.

The hydrogen yield in case of 1, 2-propane diol is much lower than for 1, 3-propanediol and this clearly indicates the occurrence of dehydration reactions. The dehydration reaction is more favourable in case of 1, 2-propanediol than 1, 3-propanediol as explained below. In case of 1, 3-propanediol, there is only one available site for dehydration reaction to occur (i.e., extraction of the hydrogen atom present at second carbon atom followed by OH removal present at β position) and there are two factors that decelerate the dehydration route; steric hindrance caused by the two OH groups that surrounds the hydrogen atom on the second carbon and the less stable radical formed in the absence of electron-releasing substituent, oxygen atom.

For dehydration reaction in case of 1, 2-propanediol there are three available sites where the hydrogen can be extracted. Extraction of any hydrogen attached to carbon atom will lead to formation of a radical in which OH is present at β position and hence the chances of OH removal and hence dehydration is more likely in the case of 1, 2-propanediol.

4. Conclusions

The influence of alkyl chain length (C₁–C₈) for two homologous series of acids and alcohols as well as the number of OH groups and their position on a C₃ backbone on the gasification behaviour in supercritical water is studied. Alcohols were found to be easier to gasify than the corresponding acids. With increasing the chain length of acids from C₁ to C₈, the gasification efficiency (GE) initially decreases drastically and then stabilizes. While formic acid converts completely to gases, the rest of acids are quite prone to conversion. Also the initial acid concentration has a high impact on the gasification efficiency. Acids with an even number of carbon atoms were found to have high GE than the adjacent odd carbon atoms. A remarkable oscillating trend for the CH₄ and C₂ yield with increasing carbon number was noticed from the experimental data, but can be understood and explained on basis of the reaction mechanisms postulated in this work, characterized by an initiation step

via O–H scissioning and subsequent β -scission reactions. Similarly, less C_2H_6 yields was observed with even numbered carbon atoms than for their adjacent odd numbered carbon atoms.

The carbon GE trend of alcohols was quite opposite to that of acids. Methanol was quite prone to gasify, while the other alcohols are easier to convert. The GE is, however, not strongly influenced by the alcohol concentration and marginal amounts of tar and char formation is noticed with higher alcohols. The electron donating nature of OH group increases the rate of gasification by stabilizing the intermediate radical formed and we found an increase in the GE with an increase in number of OH groups. Increase in the number of OH groups decreases the formation of hydrocarbons and increases CO formation, which subsequently leads to more CO_2 and H_2 . The position of OH group has no influence on the gasification efficiency. The dehydration reaction was enhanced in case of adjacent OH groups.

Acknowledgement

This project was funded by the EOS-LT program of Senter-Novem (EOS-LT 05020).

References

- [1] D. Bröll, C. Kaul, A. Kramer, P. Krammer, T. Richter, M. Jung, H. Vogel, P. Zehner, Chemistry in supercritical water, *Angewandte Chemie-International Edition* 38 (1999) 2998–3014.
- [2] E. Dinjus, A. Kruse, Hot compressed water—a suitable and sustainable solvent and reaction medium? *Journal of Physics-Condensed Matter* 16 (2004) S1161–S1169.
- [3] P.E. Savage, Organic chemical reactions in supercritical water, *Chemical Reviews* 99 (1999) 603–621.
- [4] A. Kruse, P. Bernolle, N. Dahmen, E. Dinjus, P. Maniam, Hydrothermal gasification of biomass: consecutive reactions to long-living intermediates, *Energy & Environmental Science* 3 (2010) 136–143.
- [5] J.M.L. Penninger, M. Rep, Reforming of aqueous wood pyrolysis condensate in supercritical water, *International Journal of Hydrogen Energy* 31 (2006) 1597–1606.
- [6] L. Calvo, D. Vallejo, Formation of organic acids during the hydrolysis and oxidation of several wastes in sub- and supercritical water, *Industrial & Engineering Chemistry Research* 41 (2002) 6503–6509.
- [7] C. Di Blasi, C. Branca, A. Galgano, D. Meier, I. Brodzinski, O. Malmros, Supercritical gasification of wastewater from updraft wood gasifiers, *Biomass and Bioenergy* 31 (2007) 802–811.
- [8] A. Kruse, M. Faquir, Hydrothermal biomass gasification—effects of salts, back-mixing, and their interaction, *Chemical Engineering & Technology* 30 (2007) 749–754.
- [9] J. Yu, P.E. Savage, Decomposition of formic acid under hydrothermal conditions, *Industrial and Engineering Chemistry Research* 37 (1998) 2–10.
- [10] K. Saito, T. Shiose, O. Takahashi, Y. Hidaka, F. Aiba, K. Tabayashi, Unimolecular decomposition of formic acid in the gas phase on the ratio of the competing reaction channels, *Journal of Physical Chemistry A* 109 (2005) 5352–5357.
- [11] J. Yu, P.E. Savage, Decomposition of Formic Acid under Hydrothermal Conditions, *Industrial & Engineering Chemistry Research* 37 (1998) 2–10.
- [12] T. Honma, H. Inomata, The role of local structure on formic acid decomposition in supercritical water: a hybrid quantum mechanics/Monte Carlo study, *Fluid Phase Equilibria* 257 (2007) 238–243.
- [13] W. Buhler, E. Dinjus, H.J. Ederer, A. Kruse, C. Mas, Ionic reactions and pyrolysis of glycerol as competing reaction pathways in near- and supercritical water, *Journal of Supercritical Fluids* 22 (2002) 37–53.
- [14] N. Akiya, P.E. Savage, Role of water in formic acid decomposition, *AIChE Journal* 44 (1998) 405–415.
- [15] Y. Zhang, J. Zhang, L. Zhao, C. Sheng, Decomposition of Formic acid in supercritical Water, *Energy & Fuels* 24 (2009) 95–99.
- [16] A. Kruse, K.H. Ebert, Chemical reactions in supercritical water. 1. Pyrolysis of tert-butylbenzene, *Berichte Der Bunsen-Gesellschaft-Physical Chemistry Chemical Physics* 100 (1996) 80–83.
- [17] N. Akiya, P.E. Savage, Effect of water density on hydrogen peroxide dissociation in supercritical water. 2. Reaction kinetics, *Journal of Physical Chemistry A* 104 (2000) 4441–4448.
- [18] T.I. Mizan, P.E. Savage, R.M. Ziff, Fugacity coefficients for free radicals in dense fluids: HO_2 in supercritical water, *AIChE Journal* 43 (1997) 1287–1299.
- [19] C. Wakai, K. Yoshida, Y. Tsujino, N. Matubayasi, M. Nakahara, Effect of concentration, acid, temperature, and metal on competitive reaction pathways for decarbonylation and decarboxylation of formic acid in hot water, *Chemistry Letters* 33 (2004) 572–573.
- [20] D.L. Singleton, G. Paraskevopoulos, R.S. Irwin, Rates and mechanism of the reactions of hydroxyl radicals with acetic, deuterated acetic, and propionic acids in the gas phase, *Journal of the American Chemical Society* 111 (1989) 5248–5251.
- [21] J.C. Meyer, P.A. Marrone, J.W. Tester, Acetic acid oxidation and hydrolysis in supercritical water, *AIChE Journal* 41 (1995) 2108–2121.
- [22] M. Watanabe, T. Sato, H. Inomata, R.L. Smith, K. Arai, A. Kruse, E. Dinjus, Chemical reactions of C-1 compounds in near-critical and supercritical water, *Chemical Reviews* 104 (2004) 5803–5821.
- [23] M. Watanabe, T. Iida, Y. Aizawa, H. Ura, H. Inomata, K. Arai, Conversions of some small organic compounds with metal oxides in supercritical water at 673 K, *Green Chemistry* 5 (2003) 539–544.
- [24] D.F. McMillen, D.M. Golden, Hydrocarbon bond dissociation energies, *Annual Review of Physical Chemistry* 33 (1982) 493–532.
- [25] O.F. Olaj, in: V.C.H. Bamford, C.F. Tipper (Eds.), *Comprehensive Chemical Kinetics*. Vol. 5. Decomposition and Isomerization of Organic Compounds, Elsevier Publishing Company, Amsterdam/London/New York, 1972, 1. Aufl., XVI, 779 S., zahlr. Abb., *Angewandte Chemie* 86 (1974) 712.
- [26] M. Watanabe, H. Inomata, R.L. Smith, K. Arai, Catalytic decarboxylation of acetic acid with zirconia catalyst in supercritical water, *Applied Catalysis A: General* 37 (2001) 149–156.
- [27] N. Jia, R.G. Moore, S.A. Mehta, M.G. Ursenbach, Kinetic modeling of thermal cracking reactions, *Fuel* 88 (2009) 1376–1382.
- [28] F. Jin, T. Moriya, H. Enomoto, Oxidation Reaction of High Molecular Weight Carboxylic Acids in Supercritical Water, *Environmental Science & Technology* 37 (2003) 3220–3231.
- [29] J. Abbot, P.R. Dunstan, Catalytic cracking of linear paraffins: effects of chain length, *Industrial & Engineering Chemistry Research* 36 (1997) 76–82.
- [30] G.J. DiLeo, P.E. Savage, Catalysis during methanol gasification in supercritical water, *Journal of Supercritical Fluids* 39 (2006) 228–232.
- [31] J.G. van Bennekom, R.H. Venderbosch, D. Assink, H.J. Heeres, Reforming of methanol and glycerol in supercritical water, *The Journal of Supercritical Fluids* 58 (2011) 99–113.
- [32] W. Hack, D.A. Masten, S.J. Buelow, Methanol and ethanol decomposition in supercritical water, *Zeitschrift für Physikalische Chemie* 219 (2005) 367–378.
- [33] F. Vogel, J.L.D. Blanchard, P.A. Marrone, S.F. Rice, P.A. Webley, W.A. Peters, K.A. Smith, J.W. Tester, Critical review of kinetic data for the oxidation of methanol in supercritical water, *The Journal of Supercritical Fluids* 34 (2005) 249–286.
- [34] L.T. Boock, M.T. Klein, Lumping strategy for modeling the oxidation of C1–C3 alcohols and acetic acid in high-temperature water, *Industrial and Engineering Chemistry Research* 32 (1993) 2464–2473.
- [35] N. Boukis, V. Diem, W. Habicht, E. Dinjus, Methanol reforming in supercritical water, *Industrial & Engineering Chemistry Research* 42 (2003) 728–735.
- [36] T. Arita, K. Nakahara, K. Nagami, O. Kajimoto, Hydrogen generation from ethanol in supercritical water without catalyst, *Tetrahedron Letters* 44 (2003) 1083–1086.
- [37] S. Therdtianwong, N. Srisiriwat, A. Therdtianwong, E. Croiset, Hydrogen production from bioethanol reforming in supercritical water, *The Journal of Supercritical Fluids* 57 (2011) 58–65.